

## Ultra High Spectral Resolution Satellite Remote Sounding- Results from Aircraft and Satellite Measurements

W.L. Smith<sup>1,2</sup>, D.K. Zhou<sup>3</sup>, X. Liu<sup>3</sup>, H-L. Huang<sup>2</sup>, H. E. Revercomb<sup>2</sup>, A.M. Larar<sup>3</sup>, and C. D. Barnet<sup>4</sup>

<sup>1</sup>Hampton University

<sup>2</sup>University of Wisconsin-Madison

<sup>3</sup>NASA Langley Research Center

<sup>4</sup>NOAA NESDIS

### Abstract:

Ultra high spectral resolution sounding measurements are now being obtained from the Aqua satellite Atmospheric Infrared Sounder (AIRS) fulfilling the dream of obtaining high vertical resolution temperature and moisture profiles remotely from space. The AIRS was proposed as a result of a successful aircraft demonstration of the ultra high spectral resolution sounding concept conducted from the high altitude NASA ER-2 aircraft with the High resolution Interferometer Sounder (HIS). Since that time two cross-track scanning successors to the HIS, the NAST-I (NPOESS Airborne Testbed-Interferometer) and the S-HIS (Scanning-HIS), have been flying to validate the AIRS and to pave the way for ultra high spectral resolution interferometer sounders soon to fly on the METOP and NPOESS operational satellites. This paper reviews the historical development of the ultra high spectral resolution sounding concept. AIRS and NAST-I results are shown for various validation campaigns. The Geostationary Imaging Fourier Transform Spectrometer (GIFTS), which has been developed to pave the way for the implementation of the ultra high spectral resolution sounding concept on geostationary satellites, is also discussed.

### I. Background

As shown in Figure 1, the satellite infrared sounding instrument era began with the launch of the InfraRed Interferometer Spectrometer (IRIS) and the Satellite InfraRed Spectrometer (SIRS) on the Nimbus 3 and 4 satellites (launched in 1969 and 1970, respectively). These were low spatial ( $\sim 200$  km) and moderate spectral ( $2.5\text{-}5\text{ cm}^{-1}$ ) resolution instruments that initially from Nimbus-3 viewed the satellite nadir and, in the case of Nimbus-4, also observed one field of view on each side of nadir. The Nimbus 5 satellite (launched in 1972) carried the much higher spatial resolution ( $\sim 30$  km) Infrared Temperature Profile Radiometer (ITPR), a multi-telescope filter radiometer which enabled cloud clearing, of partially-clouded fields of view, to be performed. The first operational filter wheel infrared sounding instrument was the Vertical Temperature profile Radiometer (VTPR) launched on the NOAA-2 (ITOS-D) satellite in late 1972. The contiguous spatially scanning High resolution Infrared Sounder (HIRS), which first flew on Nimbus-6 in 1975, became the NOAA operational satellite sounding instrument beginning with the TIROS-N series commencing in 1978. The HIRS will have seen more than 30 years of operational service before it is replaced by the Infrared Atmospheric Sounding Interferometer (IASI), on the European METOP satellites (2006), and the Cross-track Infrared Sounder (CrIS), on the U.S. NPP (2008) and NPOESS series of satellites (2010).

The geostationary satellite infrared sounding program began in 1980 with the launch of the VISSR Atmospheric Sounder (VAS) filter wheel instrument on the GOES-D satellite. Soon after

VAS was proposed, it was recognized that the vertical resolution provided by the filter radiometer instruments would limit its utility for storm scale weather forecasting (Smith, 1991). As a result, the very High resolution Interferometer Sounder (HIS) spectrometer instrument was developed by the University of Wisconsin and was flown on the NASA ER-2 high altitude aircraft to demonstrate that a revolutionary advance in satellite sounding vertical resolution could be obtained with instruments capable of two orders of magnitude more spectral measurements than were being obtained with filter radiometers. Thus, the HIS aircraft results became the basis for the development of the ultra high spectral resolution sounding instruments (IMG, AIRS, CrIS, IASI, GIFTS, and HES) now being flown on experimental satellites and soon to be flown continuously on next generation operational polar and geostationary satellites. Spatially scanning versions of the HIS (S-HIS and NAST-I) were developed in order to be able to validate the radiometric measurement performance and the derived product accuracy of these new ultra high spectral resolution satellite sounding instruments. Finally, the GIFTS was developed as an approach to implement the ultra high spectral resolution sounding capability on a 3-axis stabilized geostationary satellite.

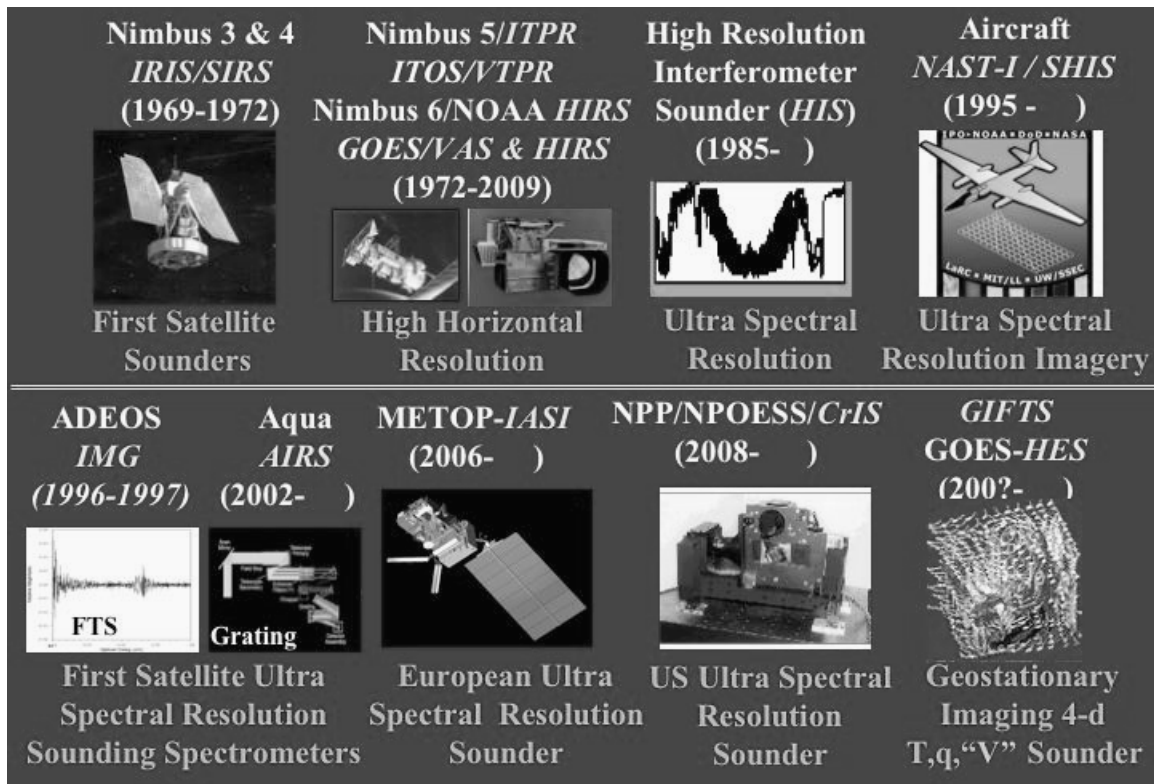


**Figure 1:** The evolution of Infrared Sounding Instruments

## II. Ultra High Spectral Resolution Sounding

Figure 2 illustrates the various spectral characteristics of the major ultra high spectral resolution sounders already designed for flight on polar and geostationary satellites. All the ultra high spectral resolution instruments are Fourier Transform Spectrometers (FTS), with the exception of the Aqua AIRS instrument, which is a large focal plane detector array grating spectrometer. The AIRS is an excellent instrument in that it is very well calibrated, has relatively low radiometric noise, and is spectrally stable, as required for obtaining high vertical resolution profile

information from its radiance observations. Unlike the grating spectrometer, the FTS uses the same detector element for observing large portions of the radiance spectrum, thereby optimizing the spectral continuity of the radiance measurements and minimizing spectrally varying calibration and co-registration error. The spectral precision and radiometric noise of the radiance measurements are the most important measurement qualities required for the retrieval of small vertical scale sounding features from radiance spectra. Small vertical structure features are extracted through a de-convolution of the spectrum of radiance, in which each spectral radiance possesses very low vertical resolving power (8-15 km). Very high spectral relative accuracy is thus required to reveal the small vertical structure (1-2 km) atmospheric features contained in the small spectral variations of radiance that they produce.

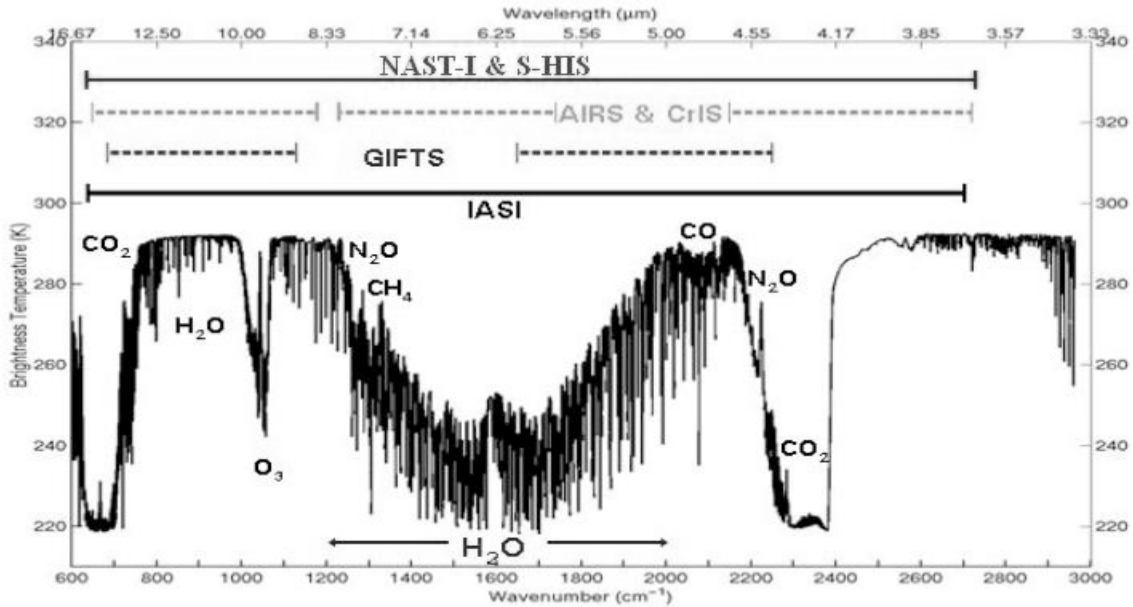


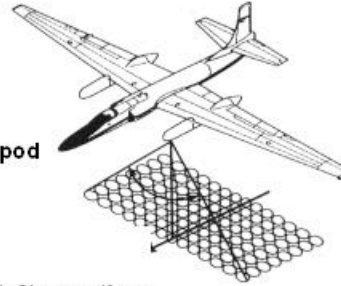
**Figure 2:** Spectral bands for aircraft and satellite ultra high spectral resolution sounding instruments

### III. The NAST-I

The NPOESS Airborne Sounder Testbed – Interferometer, NAST-I (Cousins and Smith, 1997 and Smith et. al., 1999, 2005), described in Figure 3, was developed by the National Polar-orbiting Operational Environmental Satellite System (NPOESS) Integrated Program Office (IPO) to be flown on high altitude aircraft and provide experimental observations needed for finalizing specifications and testing proposed designs and data processing algorithms for the Cross-track Infrared Sounder (CrIS). The NAST-I has a spectral range of 3.6–16.1  $\mu\text{m}$ , without gaps, and covers the spectral ranges and resolutions of all current and planned advanced high spectral resolution infrared spectrometers to fly on polar orbiting and geostationary weather satellites, including the Aqua-AIRS (Atmospheric InfraRed Sounder), METOP-IASI (Infrared Atmospheric Sounding Interferometer), the NPP (NPOESS Preparatory Project)/NPOESS CrIS (Cross-track Infrared Sounder), and the GIFTS (Geosynchronous Imaging Fourier Transform Spectrometer). The NAST-I spectral resolution ( $0.25 \text{ cm}^{-1}$ ) is equal to, in the case of IASI, or higher than all current and planned advanced sounding instruments. Thus, the NAST-I data can be used to simulate the radiometric observations to be achieved from these advanced sounding instruments. The NAST-I spatially scans the Earth and atmosphere from an aircraft, such as the high-altitude NASA ER-2 or the Northrop-Grumman Proteus research aircraft. From an aircraft altitude of 20

km, 2.6 km spatial resolution within a 40 km swath width is achieved, thereby providing three-dimensional ultra high spectral resolution images of radiance and derived geophysical products.

- **Instrument Characteristics**
  - infrared Michelson interferometer (9000 spectral channels) 3.5 – 16 microns @ 0.25  $\text{cm}^{-1}$
- **Aircraft Accommodation**
  - ER-2 Super pod & Proteus Underbelly pod
- **Radiative Measurement Capability**
  - calibrated radiances with 0.5 K absolute accuracy, 0.1 K precision



<b>Spatial Resolution</b> 130m/km flight alt. (2.6 km from 20km)
<b>Swath Width</b> 2 km /km flight alt. (40 km from 20km)

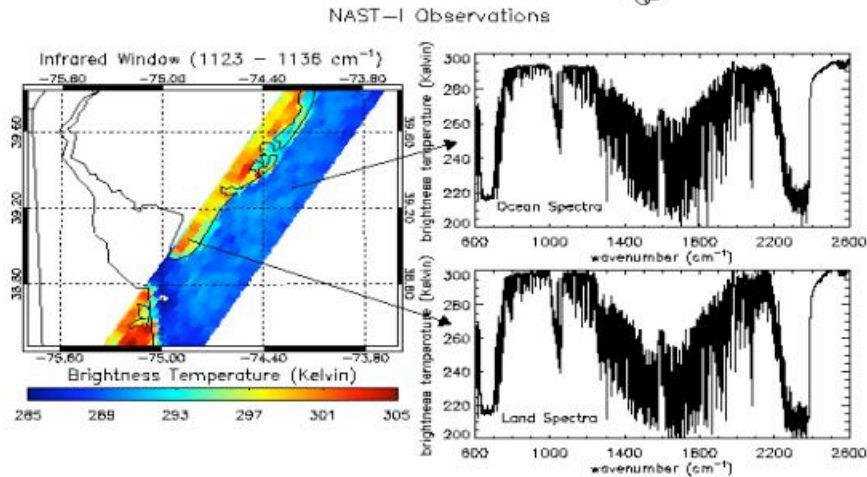


**Figure 3:** NAST-I Instrument characteristics and an example of an observed window channel image showing water and land spectra corresponding to two different scan spots.

#### IV. Atmospheric Infrared Sounder (AIRS)

The Aqua satellite AIRS instrument (Figure 4) is the first US space borne spectrometer designed to meet the 1-K/1-km sounding accuracy objective by measuring the infrared spectrum quasi-continuously from 3.7 to 15.4 microns with high spectral resolution (Aumann et. al., 2003). The sensitivity requirement, expressed as Noise Equivalent Differential Temperature (NEdT), referred to 250-K target-temperature, ranges from 0.1K in the 4.2- $\mu\text{m}$  lower tropospheric sounding wavelengths to 0.5 K in the 15- $\mu\text{m}$  upper tropospheric and stratospheric sounding spectral region. The AIRS Instrument provides spectral coverage in the 3.74  $\mu\text{m}$  to 4.61  $\mu\text{m}$ , 6.20  $\mu\text{m}$  to 8.22  $\mu\text{m}$ , and 8.8  $\mu\text{m}$  to 15.4  $\mu\text{m}$  infrared wavebands at a nominal spectral resolution of  $\nu/\delta\nu = 1200$ , with 2378 IR spectral samples and four visible/near-infrared (VIS/NIR) channels between 0.41 and 0.94 microns. Spatial coverage and views of cold space and hot calibration targets are provided by a 360-degree rotation of the scan mirror every 2.67 seconds. The AIRS ground resolutions at nadir are about 15 km and 2.5 km for the infrared and visible channel measurements, respectively, and the swath width is approximately 1650 km from the Aqua altitude of 705 km.

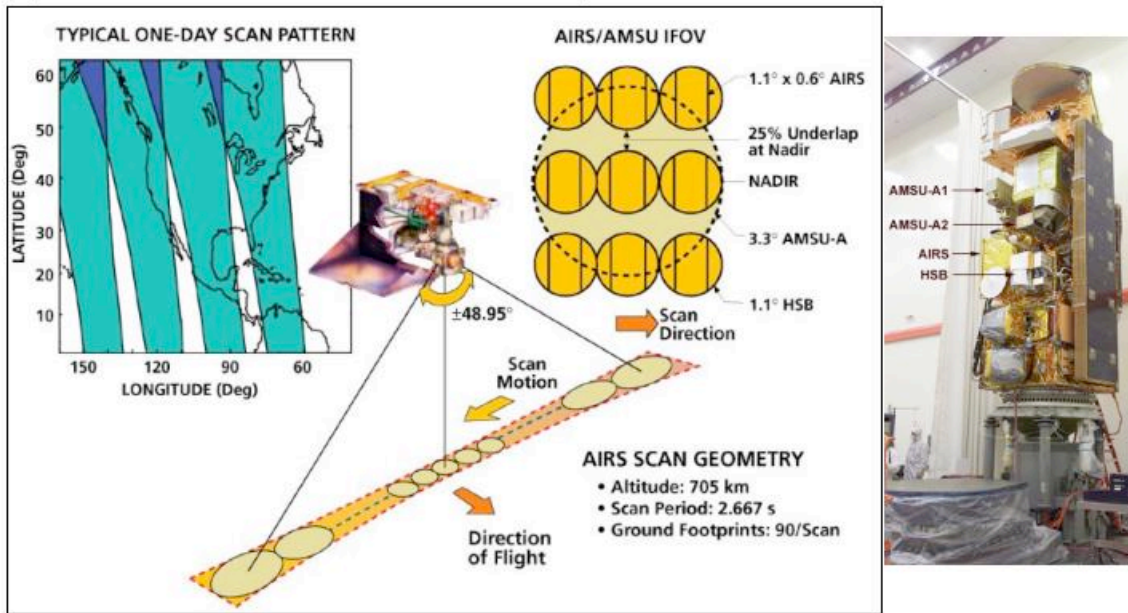


**Figure 4:** Aqua payload configuration and AIRS instrument characteristics

## V. Temperature and Moisture Retrieval Overview

In this paper, retrievals from NAST-I and AIRS using the same retrieval methodology (i.e., called the NAST-team retrieval methodology) are compared with AIRS retrievals obtained by the latest version (Version 4.0) of the AIRS science team retrieval methodology. The NAST-team and the AIRS-team retrieval methodologies are similar in that initial profiles are obtained by eigenvector regression (Zhou et. al., 2002) that are used as a first guess to a matrix inverse solution of the radiative transfer equation (Goldberg et. al., 2003, Susskind et. al., 2003, and Zhou et. al., 2005). The NAST-team radiance eigenvectors are generated from radiances calculated, using a forward radiative transfer model, from a regional and seasonal climatology of radiosonde data. For NAST-I retrievals, 4425 spectral channels are used, whereas for AIRS, 1594 spectral channels are used in NAST-team retrievals. For the AIRS-team eigenvector regression retrieval, 1688 AIRS spectral channels are used. In the case of the AIRS–team retrievals, microwave data from the AMSU instrument aboard the Aqua satellite are used to cloud clear the radiance data and provide additional sounding radiance information for the retrieval in the clouded atmosphere. The NAST-team retrieval uses only AIRS (or NAST-I) data within a retrieval procedure that directly accounts for the influence of clouds on the observed radiances, but the retrieval validity is generally restricted to above cloud top level.

Figure 5 below shows the spectral characteristics of the channels used for the NAST-team retrievals of temperature and moisture profiles from NAST-I and AIRS data. There are significant differences between the AIRS-team and the NAST-team AIRS profile retrieval approaches. For the EOF regression, the AIRS science team uses a global database of profiles extracted from ECMWF analyses co-located with actual AIRS cloud-cleared radiances. The NAST-team uses a set of regional and seasonal radiosonde profile data from which AIRS radiances are produced via radiative transfer calculation for the generation of the radiance eigenvectors. In both cases, regression coefficients are generated that relate the atmospheric state variables to the radiance eigenvector amplitudes. Also, in the physical matrix inverse retrieval step, the NAST-team uses an iterative simultaneous matrix inverse solution for all variables based

on a selection of 575 AIRS channels. The AIRS-team uses a sequential approach where 65 spectral radiances are used for temperature, 42 spectral radiances are used for water vapor, 26 spectral radiances are used for ozone, and 23 radiances are used for surface temperature. In the case of the NAST-team retrievals, surface and cloud spectral emissivity is determined by eigenvector regression and used in the matrix inverse solution. The AIRS-team retrieval surface emissivity is specified using synthetic radiance regression relationships, similar to the NAST-team retrieval (Zhou et. al., 2001) and followed by a physical approach (Susskind et. al., 2003).

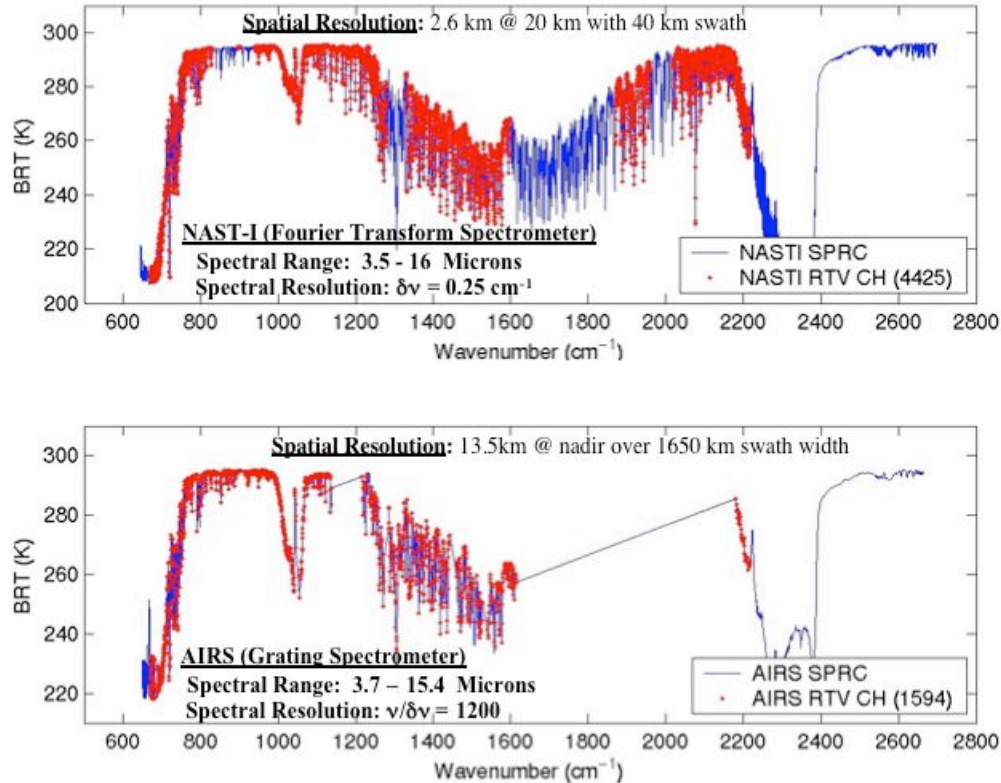


**Figure 5:** Spectral characteristics of NAST-I and AIRS and spectral channels used for NAST team retrievals of temperature and moisture retrievals.

## VI. Example Results

**Pacific THORPEX Observing System Test (PTOST):** PTOST was a field program conducted during February and March, 2003, to test certain aircraft, radiosonde, and ground systems planned to be used during the THORPEX. During PTOST, the NASA ER-2 aircraft, with the NAST-I, NAST-M (Microwave), S-HIS (Scanning-High resolution Interferometer Sounder), and CPL (Cloud Physics LIDAR) aboard, under flew the Aqua satellite in order to validate the AIRS measurement capability. Figure 6 shows a comparison of a cross section of atmospheric temperature, deviation from its level mean value, as retrieved from Aqua satellite AIRS and NAST-I radiances, observed from the ER-2 aircraft at the 20 km flight level, on March 3, 2003 near Hawaii. As can be seen, the fine scale vertical temperature profile features retrieved from the AIRS and NAST-I radiance data compare well with data from dropsondes released from the NOAA G-4 aircraft at an altitude of 13 km. (Note that for this illustration the AIRS retrievals were produced from 3 x 3 averages of spectra about their central nadir positions in order to minimize the effects of measurement noise on the retrieval of fine scale vertical temperature

structure.) The vertical resolution difference in the temperature reversal feature in the 9-10 km layer is expected due to the lower vertical resolution of the retrievals compared to the in-situ dropsonde measurements. The satellite and aircraft retrieval cross-sections show somewhat higher horizontal resolution features than those inherent in the dropsonde cross section. This is because the retrieval cross-sections are derived from relatively closely spaced retrievals (15 km for AIRS and 3 km for NAST-I), whereas the dropsonde cross-section is based on only three profiles (with about a 75 km separation distance), one at each end, and one in the middle, of the cross section shown in Figure 6. It is particularly noteworthy that the cross section mean of the AIRS and NAST-I profiles is almost identical to the mean of the dropsonde observations.

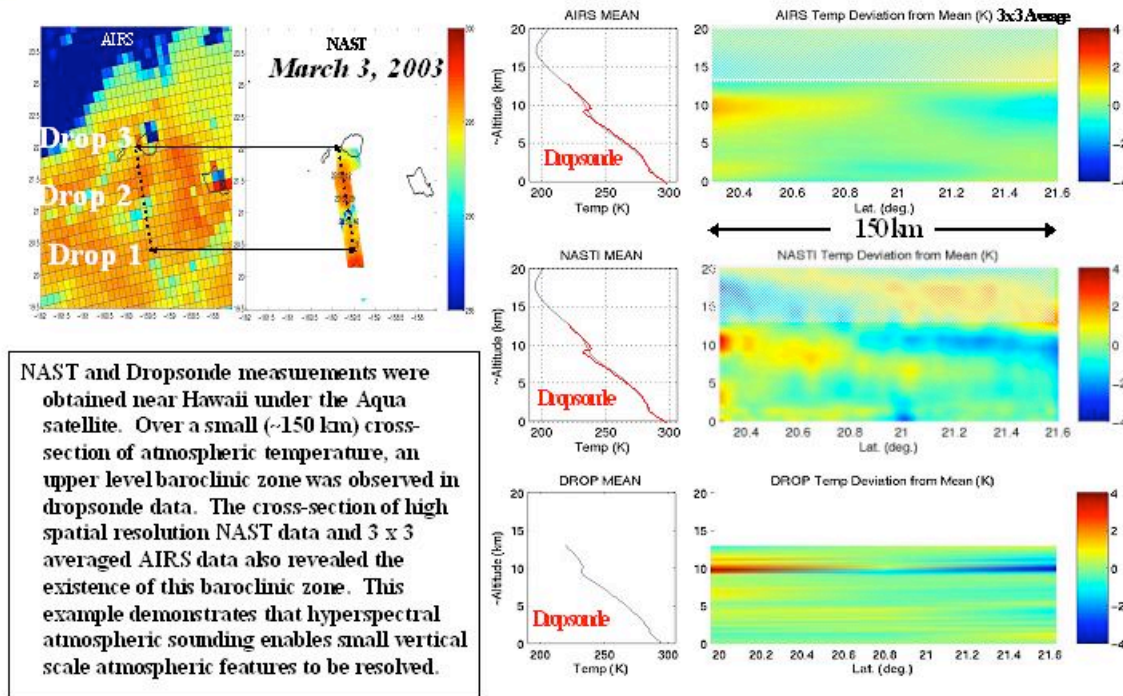



**Figure 6:** Comparison between cross sections of temperature (deviation from the level mean value) for AIRS and NAST retrievals and dropsonde observations near Hawaii on March 3, 2003. Red and Blue areas are relatively warm and cold areas, respectively.

**European AQUA Thermodynamic Experiment (EAQUATE):** The EAQUATE was held in September (2004) in Italy and the United Kingdom to demonstrate certain ground-based and airborne systems useful for validating ultra high spectral resolution sounding observations from satellites being orbited during this decade. The focus of this experiment was placed on the validation of the AIRS instrument on the EOS Aqua satellite. During the EAQUATE, the Proteus aircraft carried five separate remote sensing instruments, the NAST-I, NAST-M, S-HIS, FIRSC, and micro-MAPS. The Proteus was stationed in Naples Italy from 4 to 11 September 2004 and Cranfield England UK from 11 to 19 September 2004. During the Italian portion of the campaign (Figure 7, below), the Proteus under flew Aqua in coordination with ground-based remote sensing measurements, including several Raman LIDAR water vapor and temperature profilers and radiosondes, provided by the Istituto di Metodologie per l'Analisi Ambientale (IMAA) and the Dipartimento di Ingegneria e Fisica dell'Ambiente (DIFA), University of Basilicata in Potenza Italy. During the UK portion of the campaign (Figure 8, below), the Proteus under flights of Aqua were coordinated with the UK FAAM BAe146-301 aircraft, which flew a large payload of in-situ measurement instruments, including dropsondes, and remote sensing instruments (e.g., the

ARIES interferometer spectrometer), useful for validating the Aqua satellite observations. A total of six Proteus flights were conducted during the EAQUATE, including two under flights of Aqua during the Italian portion of the campaign and two joint Proteus and FAAM BAe146-301 under flights of Aqua during the UK portion of the campaign.


Figure 9 shows the results of an Aqua under flight conducted during the Italian portion of EAQUATE during the night of April 9, 2004. The images show the derived surface/cloud temperature retrieved for both the AIRS and the NAST-I using the NAST-team algorithm. The surface temperature is obtained when the field of view is free of cloud. Clouds exist over the sea near 38.5 N and between 40 N and 41 N latitude, the remainder of the image revealing clear sky conditions. Colder temperatures are derived over the mountainous areas of Sicily and the mainland of Italy during these near midnight observation conditions. As can be seen, there is very good agreement between the AIRS and NAST-I surface skin temperature, the major differences resulting from spatial resolution differences between the two instruments (2.5 km for the NAST-I Vs 15 km for the AIRS).

**EAQUATE (European AQUA Thermodynamic Experiment)-**  
*A project to validate radiance and geophysical products obtained by the Atmospheric Infrared Sounder (AIRS) aboard the Aqua satellite*



**Italian Campaign (Naples It., Aug. 30 – Sept. 9, 04):**

- **US Proteus Aircraft**



**NAST-I:** 3.6-16  $\mu\text{m}$ , 0.25  $\text{cm}^{-1}$

**NAST-M:** 50-425 GHz (29  $f$ 's)

**S-HIS:** 3.0-17  $\mu\text{m}$ , 0.50  $\text{cm}^{-1}$

**FIRSC:** 75-1000  $\mu\text{m}$ , 0.1  $\text{cm}^{-1}$

**$\mu$ MAPS:** 4.5-4.9  $\mu\text{m}$ , (3  $f$ 's)

- **IMAA/U of B-DIFA/U of Naples Ground-based Component**
  - **Aerosol, Raman, DIAL LIDAR:** Potenza (3) & Naples (1)
  - **Radiosondes:** Potenza, Mobile unit, Standard Network
  - **Mobile Upward-looking AERI:** 3.0-20  $\mu\text{m}$ , 1.0  $\text{cm}^{-1}$
  - **Microwave Radiometer:** 22, 31, 50-60GHz (5  $f$ 's)

**Figure 7:** The Proteus instrument payload and ground instrumentation operated during the Italian portion of the EAQUATE campaign.





**Figure 8:** The Proteus and BAe 146-130 instrument payloads flown during the United Kingdom portions of the EAQUATE.

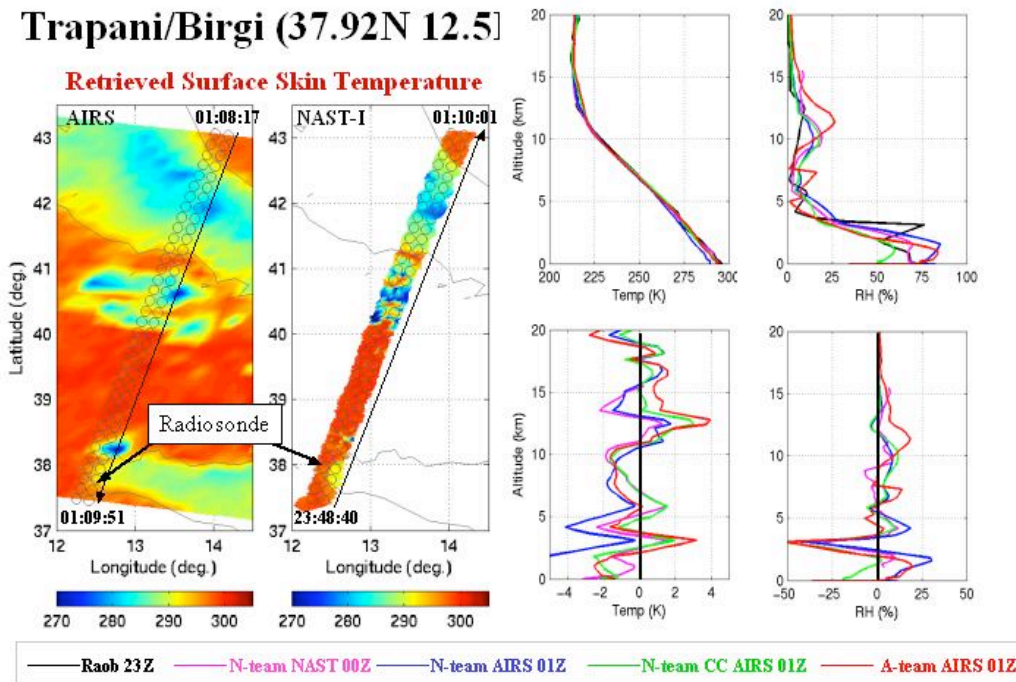


**Figure 9:** Comparisons between AIRS, AIRS/AMSU, and NAST-I retrievals with a nearly coincident Radiosonde observation. The differences between the various retrievals with the radiosonde observation are shown in the lower right hand portion of the Figure.

In Figure 9, a comparison is shown between AIRS and AIRS/AMSU retrievals obtained from cloud-cleared radiances using both the NAST-team and AIRS-team retrieval algorithms, respectively, and AIRS and NAST-I retrievals obtained from the original (not cloud-cleared) radiances using the NAST-team algorithm. A radiosonde profile is also shown for comparison with the temperature and relative humidity retrievals shown in Figure 9. As can be seen, there is very close agreement between the NAST-team retrievals for both NAST-I and AIRS and the AIRS-team AIRS/AMSU retrieval except in the 12-16 km layer for temperature and in the 0-3 km and 10-13 km layers, for relative humidity. The largest temperature disagreements with the radiosonde occur for an inversion layer near 3 km and the tropopause, near 13 km, where the differences between the retrievals with the radiosonde approach 2 K and 3 K for the NAST-I and AIRS, respectively. It can be seen from the retrieval Vs radiosonde difference plots that the vertical features of the NAST-team AIRS, AIRS-team AIRS/AMSU, and NAST-I retrievals are similar, with only a slight dependence on the retrieval methodology used. The importance of cloud-clearing is evident for this case from the comparisons for the NAST-team retrievals obtained from AIRS radiances with and without cloud-clearing.

The correspondence between the AIRS retrievals obtained using the two different retrieval methodologies (i.e., NAST-team and AIRS-team) is more clearly shown in the cross-sections presented in Figure 10. As can be seen, there is excellent correspondence between the spatial features revealed by these cross-sections, despite the significant differences between the two

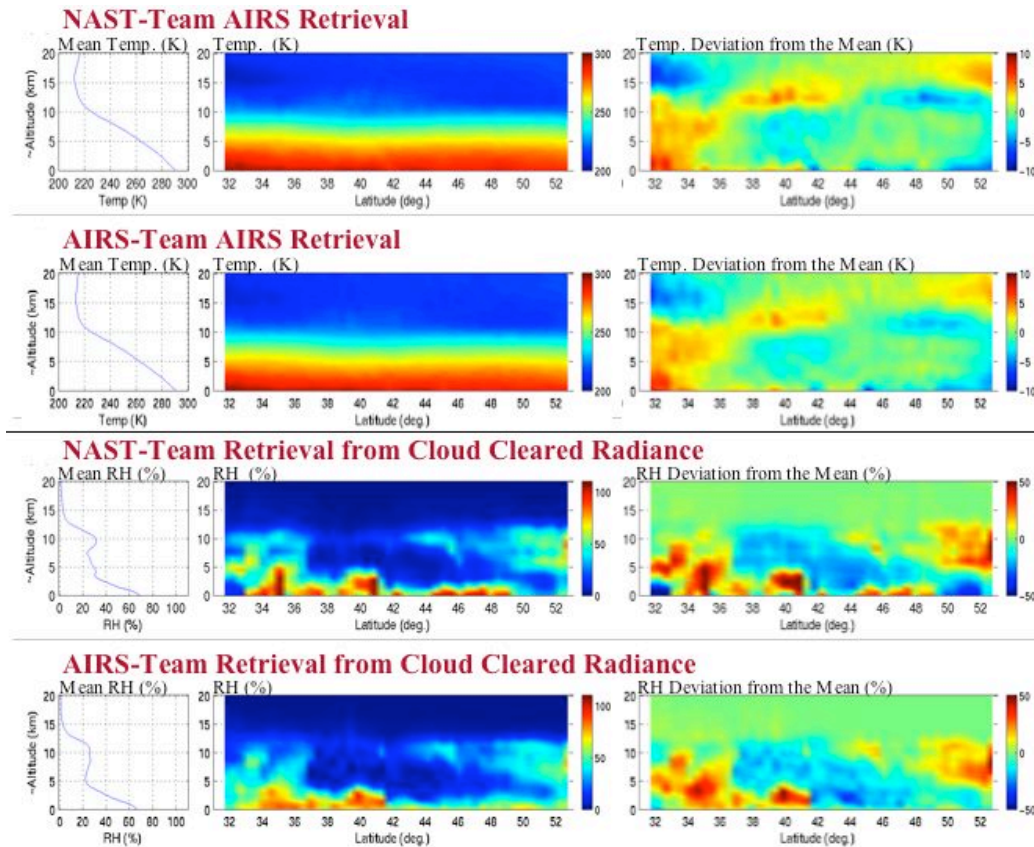


**Figure 10:** Cross-sections of temperature and relative humidity obtained from AIRS cloud-cleared radiance data using the NAST-team and AIRS-team retrieval algorithms. The deviation from the mean profile cross-sections reveal small scale features in the temperature and humidity patterns.

retrieval algorithms. It is noted, however, that slightly larger spatial gradients result with the NAST-team algorithm. The only region of significant difference is in the near surface relative humidity over Europe, between 44 N and 55 N latitude, where the NAST-team retrieval reveals much greater spatial variability, possibly a result of the difference in the manner in which surface emissivity is handled in the two different retrieval schemes.

Figure 11 shows a comparison of the NAST-team AIRS and AIRS-TEAM AIRS/AMSU temperature vertical cross-sections for two different days off the southwest coast of the United Kingdom. As can be seen, there is very close agreement between these two sets of retrievals, although there appears to be slightly more fine scale structure resolved by the NAST-team retrieval, especially for the 18 September case. The enhanced fine scale structure of the NAST-team retrieval is possibly a result of larger number of AIRS spectral channels used in the physical matrix inverse simultaneous solution, the final step of the retrieval process.

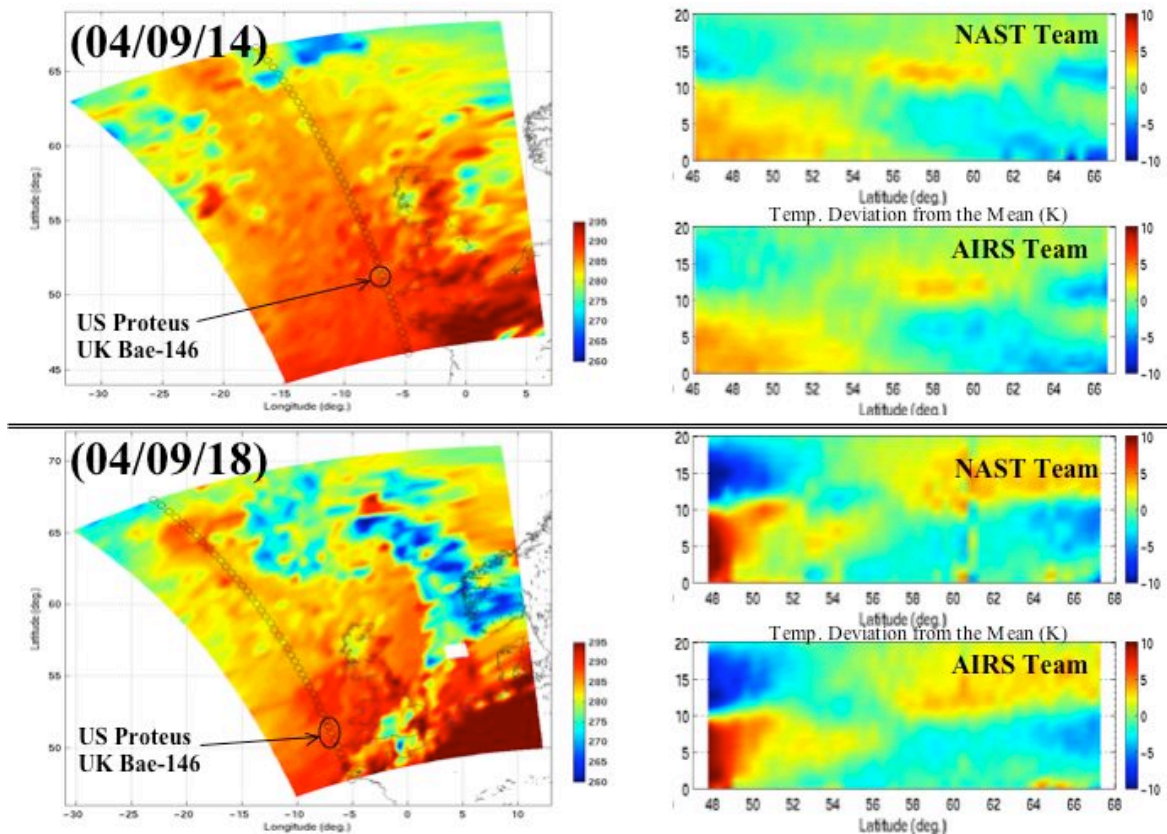


**Figure 11:** Comparison of NAST-team and AIRS-team temperature retrieval (deviations from mean profile) cross-sections along the same geographical track for September 14 and 18, 2004, off the west coast of the United Kingdom. The images on the left show the surface/cloud temperature distribution retrieved using the NAST-team algorithm.

Figure 12 shows the comparison between the AIRS-team AIRS/AMSU, NAST-team AIRS, and NAST-I temperature profile retrievals with dropsondes conducted for the area shown by the oval on the lower left hand portions of the surface/cloud temperature images shown in Figure 11. A nearby radiosonde observation is also shown in order to provide validation data above the dropsonde altitude of 6 km. It is encouraging that all the temperature sounding retrievals are in generally good agreement with each other and with the coincident dropsonde observation. This agreement can be seen in the plots of deviations of the retrieval and dropsonde values from the radiosonde observations shown in the bottom portion of this figure for the two observation days.

The biggest disagreement between the retrievals appears to be in the surface boundary layer and in the tropopause region. For the near surface boundary layer region on September 18, 2004, the NAST-I and the AIRS-team AIRS/AMSU retrievals seem to agree better with the dropsonde observations than does the NAST-team AIRS retrievals, which agree best with the radiosonde observations. The AIRS-team AIRS/AMSU retrieval seems to agree best with the radiosonde observations for the tropopause region, on these two days, possibly due to the use of the AMSU data in the AIRS-team retrieval.

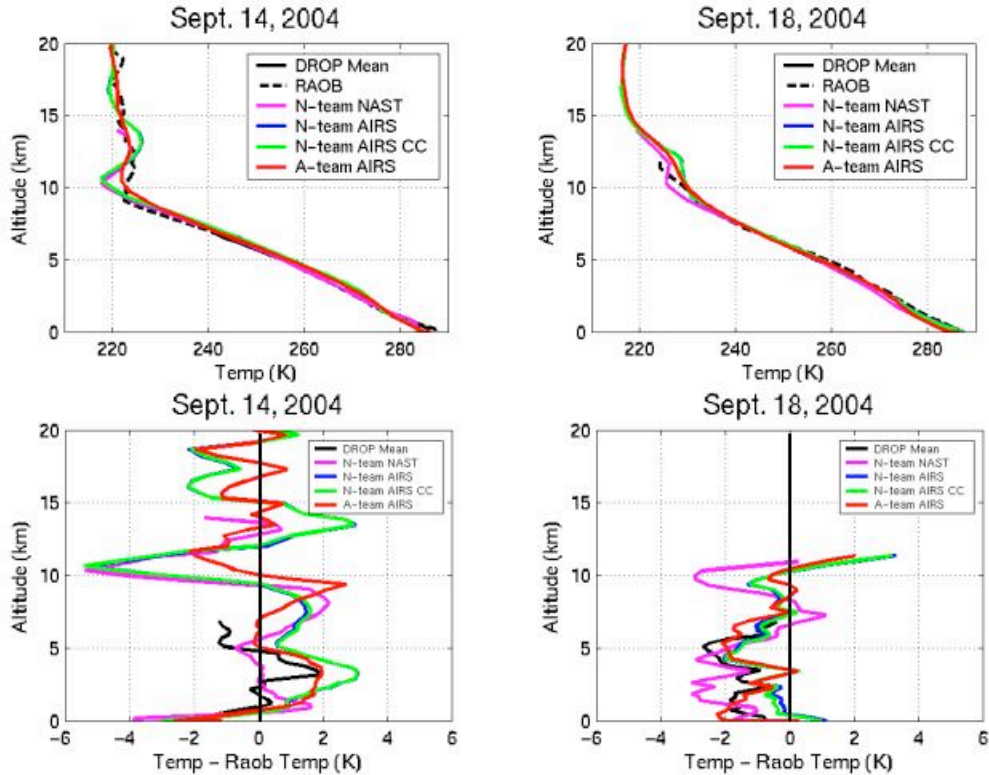


**Figure 12:** Comparison between NAST-team NAST-I and AIRS temperature retrievals and AIRS-team AIRS/AMSU retrievals with dropsonde and radiosonde observations for 14 and 18 September off the southwest coast of the United Kingdom. The deviation plots in the lower portion of this figure is respect to a nearby radiosonde observation.

Figure 13 shows a plot, similar to that shown Figure 12, but for relative humidity. As with temperature, the retrieved relative humidity profiles are in generally good agreement and in good agreement with the dropsonde observation. It is interesting that, for this case, the AIRS-team AIRS/AMSU retrieval is in relatively good agreement with the NAST-team NAST-I retrieval near the surface. The overall agreement between the AIRS-team AIRS/AMSU retrievals with the NAST-team AIRS and NAST-I retrievals and the dropsonde observations, indicates that the latest version (i.e., ver. 4.0) of the archived AIRS/AMSU retrievals are reasonably accurate, at least for the clear sky oceanic conditions considered here.

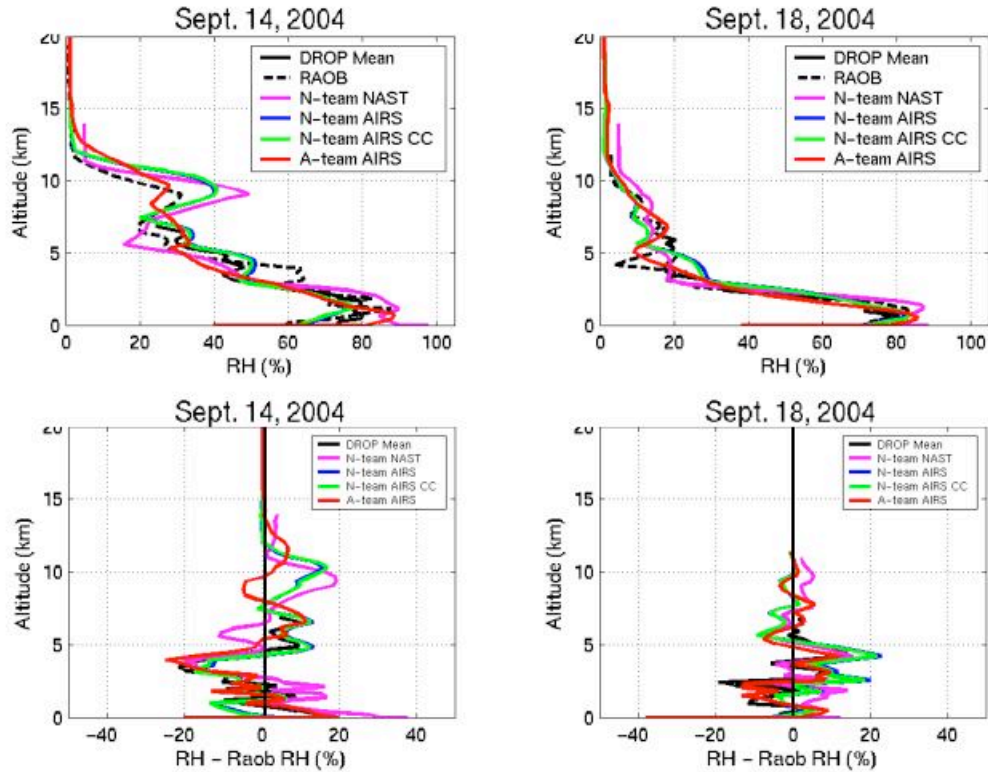


**Figure 13:** Comparison between NAST-team NAST-I and AIRS relative humidity retrievals and AIRS-team AIRS/AMSU retrievals with dropsonde and radiosonde observations for 14 and 18 September off the southwest coast of the United Kingdom. The deviation plots in the lower portion of this figure is respect to a nearby radiosonde observation.

*The Atlantic THORPEX Regional Campaign (ATReC)* was held from November 18 - December 15, 2003. The NASA ER-2 and the University of Wyoming Citation aircraft were based at Bangor, Maine. The ATReC focused on reducing the number and size of significant weather forecast errors over Europe and the eastern USA by infusing extra remote sensing and in-situ observations over sensitive (i.e. oceanic) regions. ER-2 flights contributed to ATReC by focusing on satellite sensor validation under flights (TERRA, AQUA, & DMSP).

The NASA ER-2 flew during the ATReC with an instrument payload identical to that employed during the PTOST, as described earlier. Because of the high probability of clouds over the North Atlantic Ocean during the winter months of the year, ATReC was used as an opportunity to test a new algorithm for handling clouds in the retrieval of atmospheric profiles from hyperspectral radiance measurements. The algorithm (Smith et. al., 2004, and Zhou et. al., 2005) takes advantage of the fact that clouds produce significant spectral radiance structure that depends upon their microphysical properties. Also, the height of the cloud is related to the depth of absorption line features in the emission spectrum (i.e., the lower the clouds, the greater the amplitude of the absorption line radiance features). For cloud cases, accurate atmospheric profiles are obtained down to the cloud top level. Also, if the cloud is semi-transparent or broken, the profile below the cloud level is retrieved.

The algorithm is the Empirical Orthogonal Function (EOF) regression algorithm. In this application of the algorithm, radiance eigenvectors and regression relations between atmospheric parameters and radiance eigenvector amplitudes are based upon radiative transfer calculations for

a wide variety of atmospheric temperature, moisture, and cloud profile conditions. For the radiance EOF regression training, a very large sample of radiosondes from a ten-year period is used to simulate NAST and AIRS radiances. Clouds are introduced at levels where the radiosonde humidity exceeds a threshold prescribed as a function of altitude. A physically-based cloud radiative transfer model (Huang et. al., 2002) was developed by the University of Wisconsin – CIMSS (Huang et. al., 2004) based on DISORT calculations performed for a wide variety of cloud microphysical properties by Ping Yang et. al., (2003). This model is used to account for the influence of clouds on the calculated radiance spectrum. The cloud microphysical properties are included in a realistic manner by using a statistical distribution of microphysical properties in accordance with real observations conducted over many years from aircraft and balloon (Heymsfield et al., 2003). Cloud microphysical properties were assigned to each cloudy radiosonde observation by using a random number generator to define an optical depth between 0 and 4 from a uniform distribution of the logarithm of the optical depth, and the effective particle radius was defined using a relation, provided in Table 1 below, based on the aircraft and balloon observations of Heymsfield et al. (2003). The particle radius is changed by a random amount selected from a Gaussian distribution of random numbers with a standard deviation of 10%, in order to represent the scatter of real observations. If two or more cloud layers exist, the lower level cloud is represented as an equivalent cloud-free isothermal temperature condition in the radiative transfer calculation. Thus, the statistics enable the retrieval of profiles below optically thin upper level clouds only (e.g., thin Cirrus). Regression relations are also generated for predicting cloud height, visible optical depth, and particle diameter. Because the radiance is highly non-linear with respect to cloud height, statistics are formulated for one class of data which contains all cloud height conditions and eight other height classes for which the cloud height has been stratified to within 1 km of the mean for that statistical class. The final cloud height class used for the retrievals is obtained by iteration beginning with the unclassified class to predict the initial cloud height stratification for the retrievals. Usually, the final cloud height class is defined within five iterations of the cloud height prediction process. Table 1 below summarizes the characteristics of the cloud model and the simulations of clouds as used for the EOF regression training.

In the retrieval process, there is an attempt to retrieve the correct profile below a semitransparent and/or scattered cloud layer with an effective optical depth (defined here from the product of the fractional cloud amount times the cloud visible optical depth) less than unity. If an opaque lower level cloud underlies the semitransparent and/or scattered upper level cloud, an isothermal condition will be retrieved below the lower cloud deck. EOF regression enables both the cloud height and the cloud microphysical properties of the highest-level cloud to be estimated.

Figure 14 shows a vertical cross section of temperature and moisture profiles retrieved from NASA ER-2 aircraft NAST-I data for a very cloudy situation observed over the Western Mid-Atlantic Ocean on December 3, 2003.. The retrieved cloud height is compared with that estimated from a nadir looking Cloud Physics LIDAR (CPL) on-board the ER-2 aircraft. The flight track is shown over visible and IR images obtained from the GOES spacecraft. In the retrievals shown in Figure 14, the profiles retrieved below clouds with a predicted optical depth greater than unity were considered missing since their accuracy would be degraded significantly from that achievable under cloudless sky conditions. As can be seen, there is excellent agreement between the LIDAR and NAST-I retrieved cloud heights, indicating that the retrieval of other properties, such as the cloud microphysical properties and the temperature and humidity profiles, should also be accurate. The horizontal uniformity of the retrieved temperature and humidity conditions across the wide variety of cloud height conditions indicates that this is the case.

**Table 1:** Cloud Radiative Transfer Model and Cloud Simulation Characteristics

- 
- **Perform a realistic simulation of clouds for synthetic EOF radiance training**
  - **Diagnose 0-2 cloud layers from radiosonde relative humidity profile**
    - A single cloud layer (either ice or liquid) is inserted into the input radiosonde profile.
    - Approximate lower level cloud using opaque cloud representation (i.e., isothermal/saturated)
  - **Use parameterization of Heymsfeld's\* balloon and aircraft cloud microphysical data base (2003) to specify cloud effective particle radius,  $r_e$ , and cloud optical depth,  $\tau$ , (i.e.,  $r_e = a \tau^a / [\tau - b\tau^a]$ ).**
    - Different habitats can be specified (Hexagonal columns assumed here)
    - Different clouds microphysical properties are simulated for same radiosonde using random number generator to specify visible cloud optical depth within a pre-specified range. 10 % random error added to parameterized effective radius to account for real data scatter.
  - **Use LBLRTM/DISORT "lookup table" to specify cloud radiative properties**
    - Spectral transmittance and reflectance for ice and liquid clouds interpolated from multi-dimensional look-up table based on DISORT multiple scattering calculations for the (wavenumber range 500 – 2500  $\text{cm}^{-1}$ , zenith angle 0 – 80 deg,  $D_{\text{eff}}$  (Ice: 10 – 157  $\mu\text{m}$ , Liquid: 2 – 100  $\mu\text{m}$ ),  $\text{OD}(\text{vis})$  (Ice: 0.04 - 100, Liquid 0.06 – 150)
  - **Compute EOFs and Regressions from cloudy radiance data base**
    - Regress cloud properties ( $p$ ,  $\tau$ ,  $r_e$ ) and surface and profile parameters against radiance EOFs
    - For small optical depth, output entire profile down to surface or lower opaque cloud level
    - For large upper level cloud optical depth, output profile above the upper cloud level

Heymsfeld, A. J., S. Matrosov, and B. A. Baum: Ice water path-optical depth relationships for cirrus and precipitating cloud layers. *J. Appl. Meteor.* October 2003

Evidence of the accuracy of profile conditions that can be retrieved under cloudy conditions is given by Figure 15, which shows a comparison of the EOF regression retrievals obtained from AIRS and NAST-I data in comparison to dropsonde observations made along the flight track of the ER-2. One can see generally good correspondence between the NAST and AIRS observations with the dropsondes, even though their time differences may be as large as 4 hours. However, it is also seen that the AIRS retrievals are relatively noisy (i.e., temperature retrievals varying by several degrees over short distances) as compared to the NAST retrievals. The noise in the AIRS cloudy sky retrievals may be due to false spectral features that can appear in AIRS radiance spectra observed in the vicinity of clouds. This false spectral structure is due to the fact that the radiance for each spectral position is observed by a separate detector element and the fields of view of these detector elements are not perfectly co-registered. As a result, each spectral channel observes a slightly different scene condition and this can lead to erroneous spectral structure, in the case of an inhomogeneous cloudy scene. It may be possible, through a more careful selection of the spectral channels used, to alleviate the impact detector co-registration error on the AIRS cloudy sky profile retrievals.

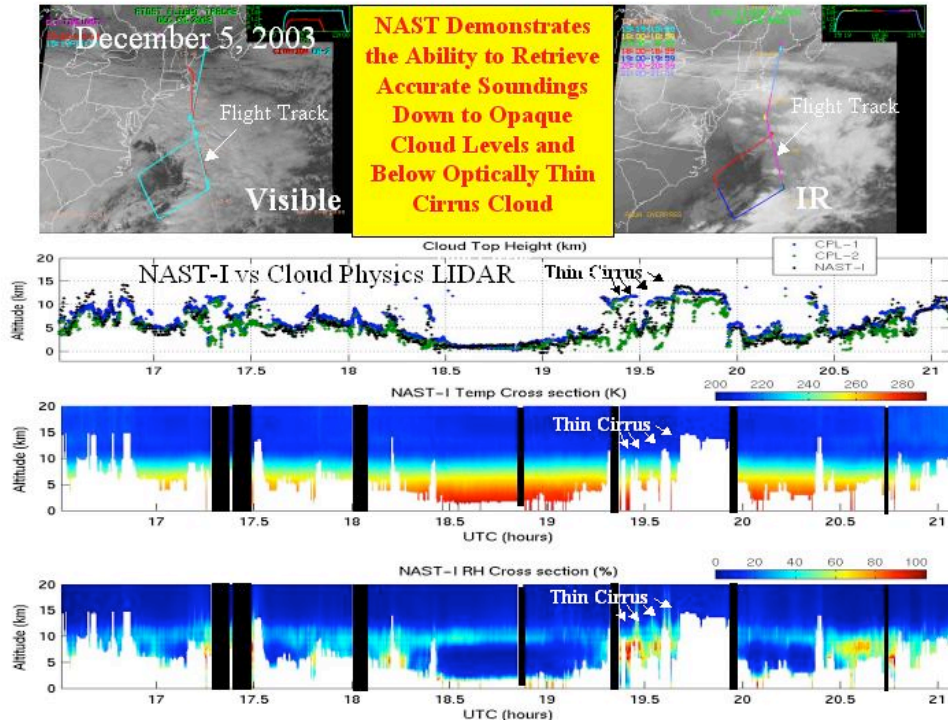


**Figure 14:** Temperature and humidity cross-sections from NAST-I cloud contaminated radiances observed along the flight track of the NASA ER-2 aircraft flying at 20km flight altitude over a wide variety of clouds.

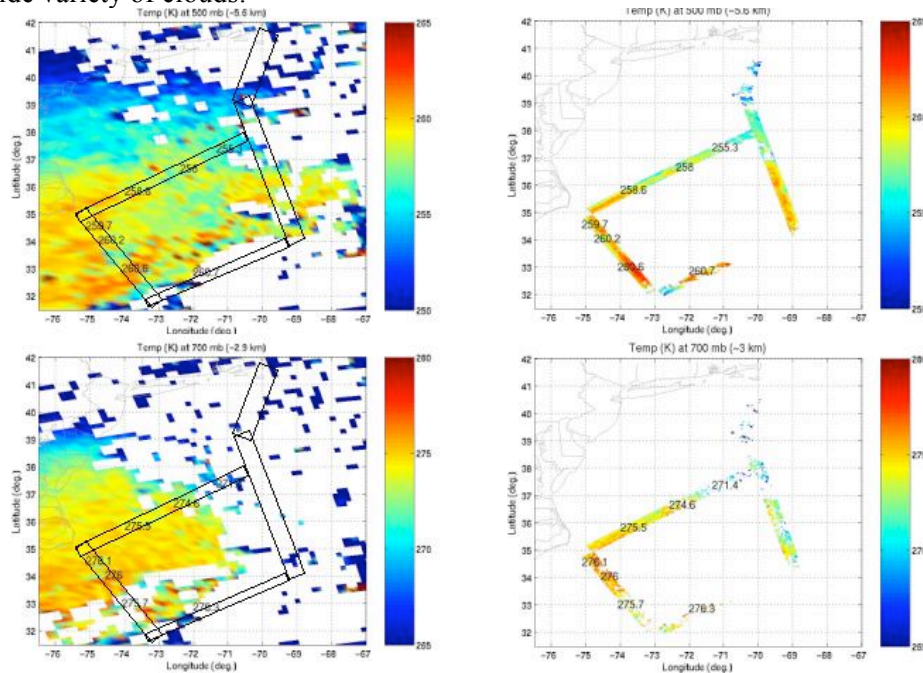


**Figure 15:** Retrievals of atmospheric temperature at 500mb and 700 MB obtained from Aqua satellite AIRS radiance spectra and NAST-I radiance spectra. Dropsondes from the NOAA Gulf stream along the track of the ER-2 aircraft are shown to validate the retrieval results.



#### IV Geostationary Ultra-spectral Instruments

Geostationary satellite ultra high spectral resolution instruments are now being studied for implementation on future operational geostationary satellites operated by the US, Europe, China, Japan, and Russia. The forerunner of these instruments is the Geosynchronous Imaging Fourier Transform Spectrometer or GIFTS (Smith et. al., 2001). The GIFTS combines a number of advanced technologies to observe atmospheric weather and chemistry variables in four dimensions. Large area format Focal Plane detector Arrays (LFPAs) provide near instantaneous large area coverage with high 2-d horizontal resolution. A Fourier Transform Spectrometer (FTS) in front of the LFPAs enables atmospheric radiance spectra to be observed simultaneously for all detector elements, thereby providing high vertical resolution temperature and moisture sounding information. The fourth dimension, time, is provided by the geosynchronous satellite platform, which enables near-continuous imaging of the atmosphere's three-dimensional spatial structure. The key advance that GIFTS, and its follow-on operational satellite versions, achieves beyond current geosynchronous capabilities is that the water-vapor winds will be altitude-resolved throughout the troposphere.

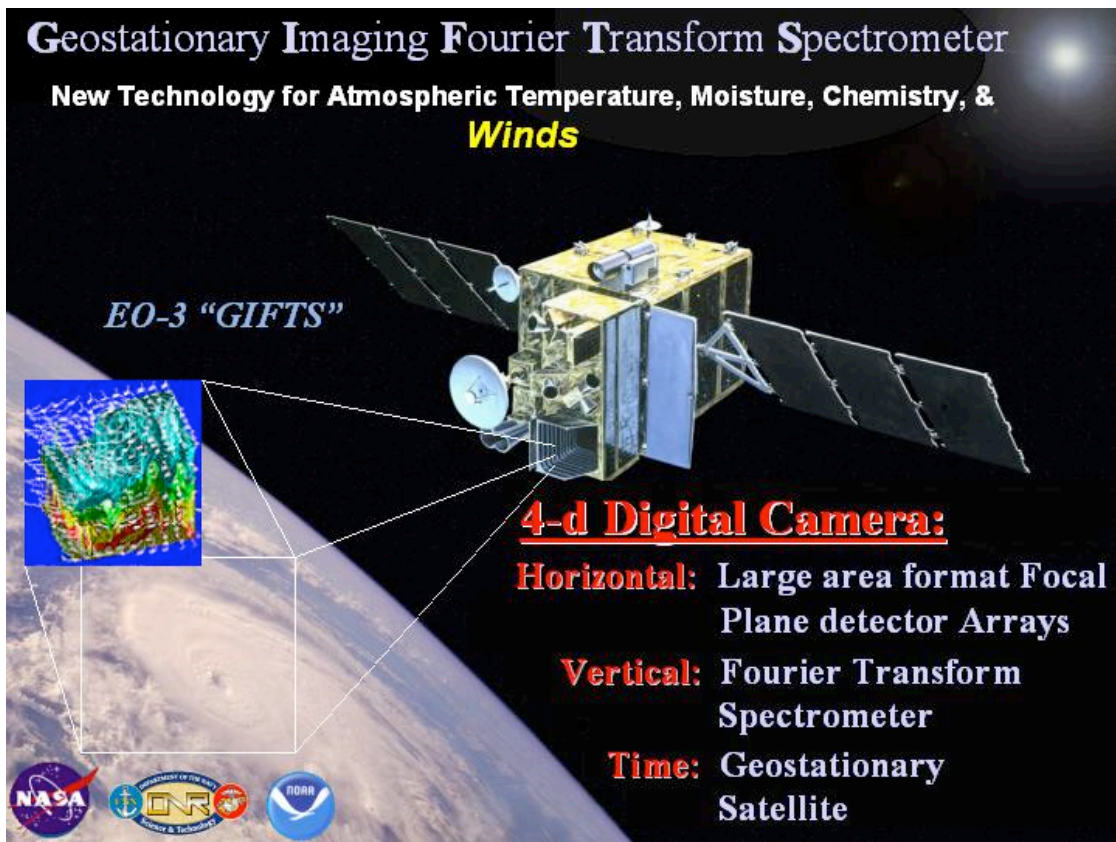


**Figure 16:** An artist conception of the GIFTS instrument aboard a geostationary satellite observing the water vapor and wind structure of a hurricane.

An ER-2 NAST-I flight off the coast of California on 11 February 2003 was coordinated with an under-flight of a Navy Twin Otter aircraft carrying the Doppler Wind LIDAR (DWL) for the purpose of validating the GIFTS wind measurement concept. The flight tracks are shown in Figure 17. Scientists at the University of Wisconsin (UW) produced winds from images of NAST-I retrieved level relative humidity analyses, using their objective cloud and water vapor

radiance feature-tracing algorithm. Since nine successive overpasses of the same domain were obtained, three independent sets of winds (each using three sequential analyses centered at 21, 22 and 23 GMT) were achieved. Coherent vectors were produced, even though the spatial domain is limited by the relatively low altitude (20 km) of the over-flight and the NAST-I scan angles. Wind profiles from the coincident DWL observations (Emmitt, personal communication) were used for validation of the UW results. Figure 18 shows that the agreement is good with maximum differences being less than 3 m/sec.

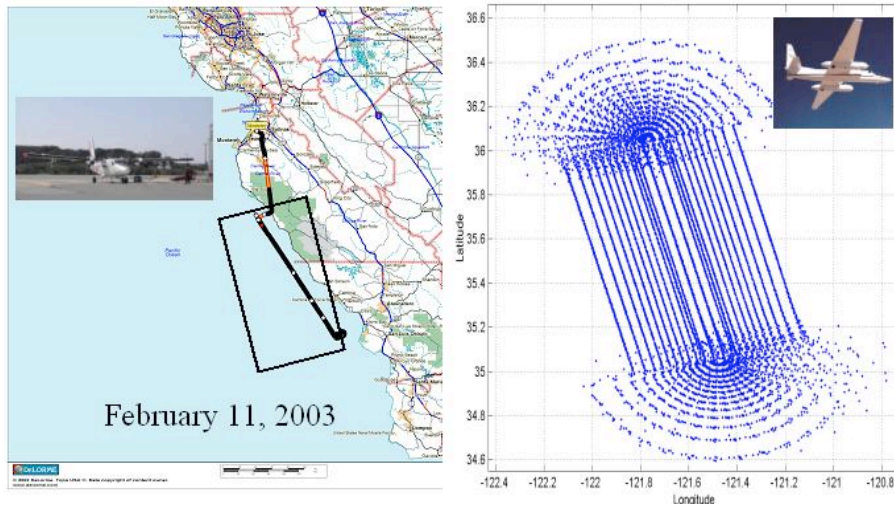


**Figure 17.** A racetrack ER-2 aircraft flight pattern was flown over the region shown this figure. This flight pattern provided multiple overpasses of the same region, and allowed sequential moisture fields to be derived for winds production. The flight path of the Navy Twin Otter, carrying the DWL, is shown on the left hand portion of this figure.

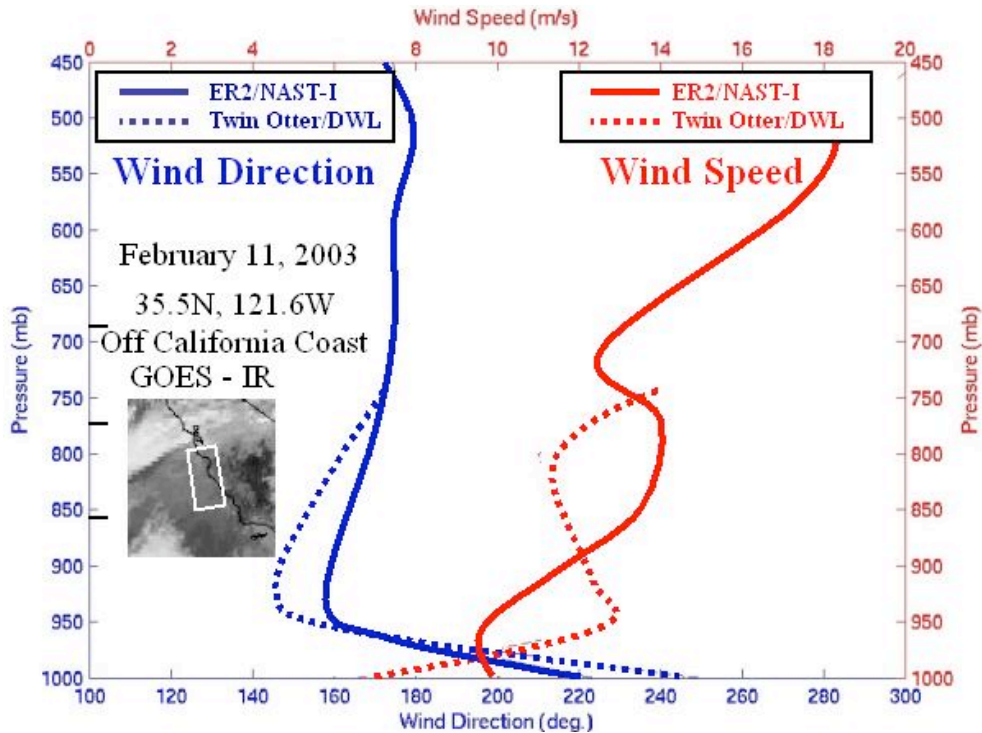


**Figure 18.** Comparison between water vapor tracer wind profiles derived from NAST-I data and coincident measurements with a Doppler wind LIDAR system.

The Space Dynamics Laboratory (SDL) of the Utah State University has completed the assembly of the GIFTS instrument as an Engineering Demonstration Unit (EDU). The GIFTS EDU is currently undergoing testing in thermal vacuum at the SDL. Assuming a successful completion of the thermal vacuum chamber testing, the instrument would be available for space qualification for flight on a future geostationary satellite mission. Such a mission is currently being pursued.

## **V. Conclusion**

Aqua satellite AIRS and airborne NAST-I ultra high spectral resolution radiance data have been analyzed to demonstrate the capabilities expected from current and future satellite ultra high spectral resolution sounding instruments. Relatively good agreement is demonstrated between the AIRS and NAST-I retrieved soundings, using two different retrieval algorithms, with dropsonde and radiosonde temperature and moisture profiles. The agreement with dropsonde observations is relatively independent of the sounding retrieval method used. The validation results obtained here provide confidence that the AIRS retrievals produced using the Version 4.0 are reasonably accurate, at least for the largely cloud free oceanic conditions considered here. It is important to note that the AIRS-team retrieval approach is in an evolutionary stage, and currently optimized for cloudy sky condition (e.g., through the use of the AMSU data). Future validation studies, using aircraft validation data sets similar to the ones used here, will focus on AIRS retrievals for cloudy sky and land surface conditions.

In conclusion, the satellite AIRS and aircraft NAST-I results shown here indicate that the next generation operational polar and geostationary satellite systems, carrying advanced ultra spectral resolution IR sounding instruments, should enable significant improvements to be achieved in global, as well as storm scale, weather predictions.

## **VI Acknowledgements**

The authors greatly acknowledge the contributions of the NASA Langley Research Center, the Space Science and Engineering Center of the University of Wisconsin – Madison, the NASA Jet Propulsion Laboratory led AIRS science team, the Instituto di Meteorologie per l'Analisi Ambientale, the United Kingdom Meteorological Office, the NASA Goddard Space Flight Center, and the NOAA National Environmental Satellite Data and Information Service for providing the data used in this study. The Integrated Program Office (IPO) for the NPOESS supported the work reported here. The personnel from these institutions who contributed to this study are too numerous to mention by name, nonetheless their personal contributions are greatly appreciated.

## **VII References**

- Smith, W. L., 1991: Atmospheric soundings from satellites - false expectation or the key to improved weather prediction? Royal Meteorological Society, Symons Memorial Lecture, London, UK, May 16, 1990. *J. Roy. Meteor. Soc.*, 117, 267-297.
- Cousins, D. and W. L. Smith, 1997: National Polar-Orbiting Operational Environmental Satellite System (NPOESS) Airborne Sounder Testbed-Interferometer (NAST-I), in *Proceedings*,

*SPIE Application of Lidar to Current Atmospheric Topics II*, A. J. Sedlacek, and K. W. Fischer, Eds., 3127, 323–331.

Smith, W.L., A. M. Larar, D. K. Zhou, C. A. Sisko, J. Li, B. Huang, H. B. Howell, H. E. Revercomb, D. Cousins, M. J. Gazarik, D. Mooney, “NAST-I: results from revolutionary aircraft sounding spectrometer”, in *Proceedings, SPIE Optical Spectroscopic Techniques and Instrumentation for Atmospheric and Space Research III*, A. M. Larar, Ed., 3756, 2–8, 1999.

Smith, W.L., D.K. Zhou, A.M. Larar, S.A. Mango, H.B. Knuteson, H.E. Revercomb, and W. L. Smith Jr., 2005: “The NPOESS Airborne Testbed Interferometer – Remotely Sensed Surface and Atmospheric Conditions during CLAMS” *J. Atmos. Sci.*, 62, 1118 – 1134.

Aumann, H. H., M. T. Chahine, C. Gautier, M. D. Goldberg, E. Kalnay, L. M. McMillin, H. Revercomb, P. W. Rosenkranz, W. L. Smith, D. H. Staelin, L. L. Strow, and J. Susskind, 2003: AIRS/AMSU/HSB on the Aqua Mission: Design, Science Objectives, Data Products, and Processing Systems. *IEEE Transactions on Geoscience and Remote Sensing*, Vol. 41 No. 2, pp 253-264 February 2003..

Goldberg, M.D., Y. Qu., L.M. McMillin, W. Wolf, L. Zhou, M. Divakarla, 2003: “AIRS near real-time products and algorithms in support of operational numerical weather prediction,” *IEEE Transactions on Geoscience and Remote Sensing*, Vol. 41, No. 2. pp 379-389, February 2003.

Susskind, J., C. Barnet, and J. Blaisdell. "Retrieval of Atmospheric and Surface Parameters from AIRS/AMSU/HSB Data in the Presence of Clouds", 2003: *IEEE Transactions on Geoscience and Remote Sensing*, Vol. 41, No. 2, February 2003.

Zhou, D. K., W. L. Smith, J. Li, H. B. Howell, G. W. Cantwell, A. M. Larar, R. O. Knuteson, D. C. Tobin, H. E. Revercomb, and S. A. Mango, “Thermodynamic product retrieval methodology for NAST-I and validation,” *Applied Optics*, 41, 6,957–6,967, 2002.

Zhou, D. K., W. L. Smith, X. Liu, J. Li, A. M. Larar, and S. A. Mango (2005), Tropospheric CO observed with the NAST-I: retrieval methodology, analyses, and first results, *Applied Optics*, 44, 3032–3044.

Zhou, D.K., W. L. Smith, and A. M. Larar, “Surface temperature and emissivity from airborne measurements of IR radiance spectra”, *Eos Trans. AGU*, 82(47), 2001.

Smith, W. L., and D. K. Zhou, H-L Huang, Jun Li, X. Liu, and A. M. Larar, 2004: “Extraction of Profile Information from Cloud Contaminated Radiances”, Proceedings of the ECMWF Workshop on the Assimilation of High Spectral Resolution Sounders in NWP, June 28 – July 1, 2004.

Zhou, D. K., W. L. Smith, X. Liu, A. M. Larar, H.-L. A. Huang, J. Li, M. J. McGill, and S. A. Mango (2005), Thermodynamic and cloud parameters retrieval using infrared spectral data, *Geophys. Res. Lett.*, 32, L15805, doi:10.1029/2005GL023211.

H-L Huang and W. L. Smith, 2004: “Apperception of Clouds in AIRS Data”, Proceedings of the ECMWF Workshop on the Assimilation of High Spectral Resolution Sounders in NWP, June 28 – July 1, 2004.

Yang, P., B. C. Gao, B. A. Baum, Y. Hu, W. Wiscombe, S.-C. Tsay, D. M. Winker, S. L. Nasiri, 2001: Radiative Properties of cirrus clouds in the infrared (8-13 um) spectral region, *J. Quant. Spectros. Radiat. Transfer*, 70, 473-504.

Heymsfield, Andrew J.; Matrosov, Sergey, and Baum, Bryan. "Ice water path-optical depth relationship for cirrus and deep stratoform cirrus cloud layers". *Journal of Applied Meteorology* v.42 , no.10, 2003, pp1369-1390. Re

# Proceedings of the Fourteenth International TOVS Study Conference

Beijing, China  
25-31 May 2005

